

Preparation and Characterization of Vanadium Oxide Deposited on Thermally Stable Mesoporous Titania

Y. Segura,^{*,†} L. Chmielarz,[‡] P. Kustrowski,[‡] P. Cool,[†] R. Dziembaj,[‡] and E. F. Vansant[†]

Department of Chemistry, Laboratory of Adsorption and Catalysis, University of Antwerp, Universiteitsplein 1, B-2610 Wilrijk, Belgium, and Faculty of Chemistry, Jagiellonian University, Ingardena 3, 30-060 Krakow, Poland

Received: June 30, 2005; In Final Form: November 2, 2005

Vanadium oxide was deposited on mesoporous titania by the molecular designed dispersion method to investigate the potential properties of these catalysts. Mesoporous titania was synthesized following the evaporation-induced self-assembly (EISA) method with a subsequent treatment with ammonia to increase the thermal stability. As a result, the mesoporous titania obtained shows a high surface area ($\sim 350 \text{ m}^2/\text{g}$) and high stability. Vanadium oxide was deposited by the MDD method using a vanadyl acetylacetonate complex that was transformed into VO_x after a controlled calcination in air flow at 300°C . The mesostructure and porosity characteristics of titania remain even until the maximum V-loading was reached (0.4 mmol/g), as it was shown by N_2 sorption measurements at -196°C . The catalysts were characterized by chemical analysis, Fourier transform infrared-photoacoustic spectroscopy (FTIR-PAS), UV–vis diffuse reflectance (DR), and Fourier transform Raman spectroscopy. Raman spectra showed isolated V species for the different V-containing catalysts. Furthermore, UV–vis–DR revealed a higher contribution of polymeric species as the V loading increases. The $\text{VO}_x/\text{mesoporous titania}$ catalysts were highly active in the selective catalytic reduction of NO_x . A high activity in the NO conversion was observed, which increases with increasing metal loading.

1. Introduction

Supported vanadia catalysts are widely used for a large number of oxidation–reduction reactions such as the partial oxidation of organic compounds,^{1–4} aromatic compounds,^{5,6} olefins,⁷ the ammoxidation of aromatic hydrocarbons,⁸ and the selective catalytic reduction (SCR) of NO_x .^{9–13}

In particular, vanadia presents interesting properties for the SCR reaction when it is supported on TiO_2 . Among the common crystalline forms of titania, anatase is generally recognized to be the best support. However, the use of TiO_2 as a catalyst is limited by the fact that it possesses a relatively low specific surface area. Therefore, many attempts have been performed in order to synthesize mesoporous titania with a high surface area and high stability using a variety of different templates.^{14–16} Stucky et al.¹⁷ introduced a synthetic approach to mesoporous metal oxides by the so-called evaporation-induced self-assembly process (EISA). By slow alcohol evaporation, a controlled building of an inorganic network with nanocrystalline domains around the voids of the liquid–crystalline interphase results in a hexagonally ordered TiO_2 mesophase. A controlled thermal treatment in order to remove the template is crucial as it often results in a collapse of the mesoporous structure. Recently, Cassiers et al.¹⁸ developed a new synthesis step that controls the transformation into the anatase phase without loss of porosity, by treating the titania hybrid with an aqueous $\text{NH}_4\text{-OH}$ solution. This treatment results in a thermally stable mesoporous titania structure with anatase nanoparticles in the walls. The obtained mesoporous titania samples exhibit a high

surface area, which could reach $\sim 600 \text{ m}^2 \text{ g}^{-1}$, and pore volumes up to $0.30 \text{ cm}^3 \text{ g}^{-1}$. Moreover, the mesoscale order of NH_3 -treated titanias was stable after thermal treatment up to 500°C .

It is known that the catalytic activity of vanadium catalysts not only depends on the V loading but also on the structure and dispersion of the vanadium species. These factors are highly influenced by the nature of the oxide support. Therefore, it is important to investigate the properties of the transition metal oxide supports. Although in the literature, an extensive research has been done on vanadia–silica materials systems, mesoporous transition-metal oxides have been rarely studied as a support.

In this work, mesoporous titania was prepared following the post NH_3 treatment,¹⁸ which has, based on its porosity characteristics, a large potential as a catalytic support. Vanadium oxide was deposited on the mesoporous titania by means of the molecular-designed dispersion (MDD) method using vanadyl acetylacetonate (acac) complex as the vanadium source. Following the MDD method, metal acac complexes are reacted with the hydroxyls of the support material and converted into the metal oxide form after calcination.^{19–22} This method allows the vanadium oxide to be spread out on the titania support material using the bulky vanadyl acetylacetonate complexes. After deposition, a careful and controlled calcination is performed in order to remove the organic acac ligands, without collapsing the mesostructure of the support. A detailed characterization of the $\text{VO}_x/\text{mesoporous TiO}_2$ catalyst is obtained by Fourier transform infrared-photoacoustic spectroscopy (FTIR-PAS), FT Raman, UV–vis diffuse reflectance (DR), chemical analysis, and N_2 sorption measurements.

2. Experimental Section

2.1. Synthesis of Mesoporous Titania. Mesoporous titania was prepared using cetyltrimethylammoniumbromide (CTABr)

* To whom correspondence should be addressed. E-mail: yolanda.segura@ua.ac.be. Tel.: +32-3-820.23.80. Fax: +32-3-820.23.74.

[†] University of Antwerp.

[‡] Jagiellonian University.

as a surfactant and titanium tetraisopropoxide ($\text{Ti}(\text{O}^i\text{Pr})_4$) as a titanium source. The samples were synthesized following a method based on the EISA procedure.²³ $\text{Ti}(\text{O}^i\text{Pr})_4$ was added to an ethanolic HCl, resulting in a titanium precursor solution, which was added to an ethanolic CTABr solution. After vigorous stirring, the resulting solution was transferred in an open Petri dish for 7 days at 60 °C to evaporate the solvent. The molar ratios were $\text{Ti}:\text{CTABr}:\text{HCl}:\text{H}_2\text{O}:\text{EtOH} = 1:0.16:1.4:17:20$.

The mesoporous titania samples were NH_3 treated for 48 h in a reflux system. NH_4OH was added to pure water until a pH of 9–10. One gram of sample, which was aging in a Petri dish, was then treated with 50 mL of the basic water, and the pH was again brought to a value between 9 and 10. The pH was kept constant at 9–10 by the drop addition of NH_4OH .¹⁸

2.2. Metal Deposition. Vanadium metal oxide was deposited on the mesoporous titania material by the MDD. The MDD method was carried out in a liquid phase, using the vanadyl acetylacetonate complex ($\text{VO}(\text{acac})_2$) as the vanadium source and toluene as a solvent.

An amount of $\text{VO}(\text{acac})_2$ was dissolved in 100 mL of zeolite dried toluene. The dried mesoporous titania support was then added, and the solution was stirred for 1 h. After reaction, the modified support was filtered off, washed a few times with toluene, and dried under vacuum. The reaction was carried out at room temperature and in the absence of air.

The mesoporous titania materials with adsorbed complexes obtained from the liquid phase are called the precursors. The acac ligands were removed by calcination, which was performed in an oven under an air flow at 300 °C for 2 h, resulting in a final supported vanadium oxide catalyst.

2.3. Catalyst Characterization. The concentration of vanadium on the support was determined by UV–vis spectrophotometry after destruction of the samples and measured colorimetrically. The measurements were performed on a Unicam 8700 UV–vis spectrometer.

The samples were stirred for 20 min in hot sulfuric acid (2.5 M). After filtration H_2O_2 was added, and the vanadium concentration was measured at 450 nm.²⁴

FTIR–PAS were recorded on a Nicolet 20 SX spectrometer, equipped with a McClelland photoacoustic cell under dry conditions. About 1000 scans were taken with a resolution of 8 cm^{-1} . The PAS spectrometer was placed in an isolated bench, which was constantly purged with dry nitrogen to ensure complete dry conditions.

Transmission spectra were measured on a Nicolet 20 SX spectrometer equipped with a vacuum system cell and a DTGS detector and using a home-built in situ vacuum IR transmission cell. Self-supporting disks of 20 mg/cm^2 were used. A total of 100 scans were measured with a spectral resolution of 4 cm^{-1} .

FT Raman spectra were recorded on a Nicolet Nexus FT Raman spectrometer with a Ge detector. All samples were measured at room temperature in a 180° reflective sampling configuration, with a 1064-nm Nd:YAG excitation laser. A total of 2000 scans were averaged for each spectrum and the laser power was set between 1 and 2 W.

Porosity and surface area studies were performed on a Quantachrome Autosorb 1 MP instrument. N_2 adsorption–desorption isotherms were recorded at –196 °C. The Brunauer–Emmett–Teller (BET) model was used to determine the specific surface area. Total pore volume was calculated by means of the total amount of adsorbed gas at $P/P_0 = 0.95$. The samples were outgassed overnight at 200 °C.

Surface acidity of the samples was studied by the temperature-programmed desorption of ammonia (NH_3 -TPD). The measurements were performed in a flow microreactor system equipped with a QMS detector (VG Quartz). Prior to the ammonia sorption, the sample was outgassed in a flow of pure helium at 450 °C for 1 h. Subsequently, the microreactor was cooled to 70 °C, and the sample was saturated in a flow of a gas mixture containing 1 vol. % of NH_3 in helium for about 30 min. Then, the catalyst was purged in a helium flow until a constant baseline level was attained. Desorption was carried out with a linear heating rate (10 °C/min) in a flow of He (20 mL/min). Traces of H_2O and O_2 in pure helium (grade 5) used as the eluant gas were removed by appropriate traps (Alltech). Calibration of the QMS with commercial mixtures allowed to recalculate the detector signal into the rate of NH_3 desorption.

2.4. Catalytic Tests. The catalytic experiments have been performed at atmospheric pressure in a fixed-bed flow reactor (inside diameter, 7.0 mm; length, 240 mm). The reactant concentrations were continuously measured using a quadrupole mass spectrometer (VG QUARTZ) connected to the reactor via a heated line. Prior to the reaction each sample of the catalyst was outgassed in pure helium at 200 °C for 30 min. Samples of 100 mg of the catalyst were used. At the reactor inlet, the composition of the gas mixture was $[\text{NO}] = [\text{NH}_3] = 2500$ ppm, $[\text{O}_2] = 2.5\%$, and He as a balancing gas at a total flow rate of 40 mL/min. The reaction was studied at temperatures ranging from 100 to 550 °C. The intensities of the mass lines corresponding to all reactants and products were measured at a given temperature for 15–30 min after the reaction had reached a steady state. The signal of the helium line served as the internal standard to compensate small fluctuations of the operating pressure. The sensitivity factors of the analyzed lines were calibrated using commercial mixtures of gases. The possible changes in the molar flow caused by the NO and NH_3 conversion were negligible in the diluted reaction mixtures. The differences in the composition of the reaction mixture measured in the reactor inlet and outlet were used for the determination the conversion of the reactants.

The influence of H_2O on the course of the NO SCR reaction was studied by a periodical addition of water vapor into the reaction mixture. In the gas-supplying system there were two separated helium lines, first with pure helium and second with He constantly flowing through the saturator kept at 0 °C. Water vapor concentration in the reaction mixture was measured as 0.30 vol. %. The helium (used as a balance gas) was switched by means of a 4-port valve from dry to wet in intervals of 30 min. All the gas lines were heated in order to prevent condensation of water.

The influence of SO_2 on the performance of the studied catalysts was pretreatment of the outgassed sample in the flow (20 mL/min) of gas mixture containing 0.2 vol. % of SO_2 in helium and subsequent catalytic test at constant temperature. The results of catalytic measurements performed over the SO_2 -treated catalyst were compared with those obtained for the fresh sample.

An additional test presenting the activity of the VO_x mesoporous TiO_2 -based catalyst in oxidation of SO_2 to SO_3 was performed. Prior to the test, the catalyst sample (100 mg) was outgassed in a flow of helium at 400 °C. Then, the flow of helium was exchange for a flow of gas mixture containing 4 vol. % of O_2 in He. After about 50 min additional SO_2 (500 ppm) was added into the reaction mixture. The total flow rate of both gas mixtures was 50 mL/min.

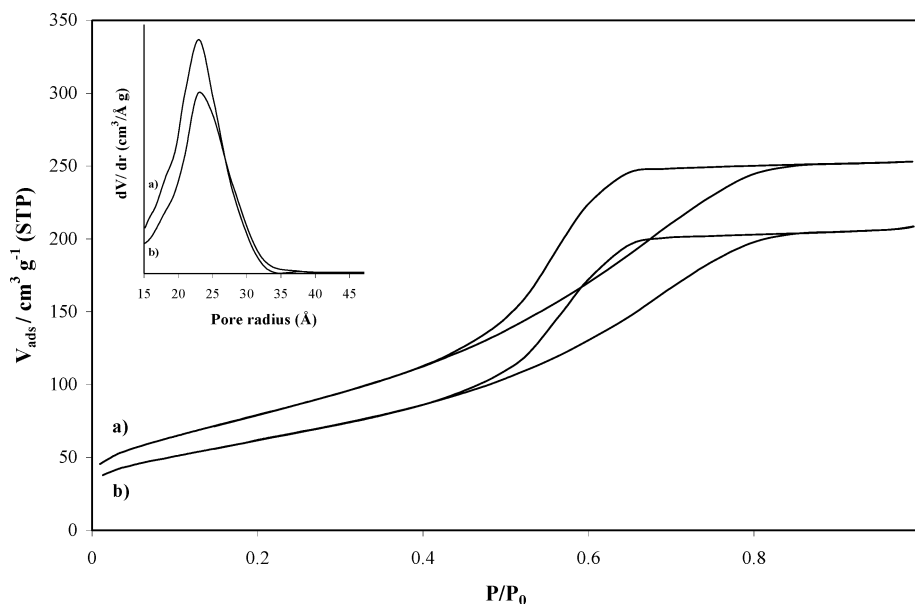


Figure 1. Nitrogen adsorption–desorption isotherms at $-196\text{ }^{\circ}\text{C}$ of mesoporous titania samples. (a) Pure mesoporous TiO_2 support; (b) $\text{VO}_x/\text{meso TiO}_2$ sample calcined at $300\text{ }^{\circ}\text{C}$ in air flow. The inset shows the corresponding mesopore size distributions.

TABLE 1: Porosity Characteristics of Various Mesoporous Titania Catalysts with Different V Loadings

catalyst	metal loading (mmol/g)	S_{BET} loss (m^2g^{-1}) %	total pore vol. (mL/g)	metal atoms/ nm^2
(1) $\text{VO}_x/\text{meso Ti}$	0.10	242 (255) 5.1%	0.36 (0.36)	0.24
(2) $\text{VO}_x/\text{meso Ti}$	0.36	260 (304) 14.5%	0.31 (0.35)	0.71
(3) $\text{VO}_x/\text{meso Ti}$	0.40	252 (345) 27.0%	0.29 (0.35)	0.70

3. Results and Discussion

Following the MDD method, the surface of mesoporous titania was modified with different amounts of vanadium, using vanadyl acetylacetonate complex as the vanadium source.

Between brackets the S_{BET} and total pore volume of the blank mesoporous titania support.

Table 1 shows the porosity characteristics and final V loading of the different catalysts. Increasing the concentration of V-acac, the final loading also increases until a maximum coverage of around 0.4 mmol/g . This maximum is due to the limited solubility of the vanadium acac complex in toluene and to steric hindrance of the V-acac complex in the mesoporous TiO_2 . V-acac deposited on SBA-15 silica support at room temperature has also a maximum loading reaching $\sim 0.4\text{ mmol/g}$.²⁵ However, it is obvious that V is more reactive toward the titania surface than to the silica surface, considering the lower specific surface area of the mesoporous titania compared to the SBA-15 material ($\sim 700\text{ m}^2/\text{g}$). On silica, this results in a lower number of metal atoms per nm^2 , 0.08, 0.30, and 0.33 V atoms/nm^2 for a V loading of 0.10, 0.36, and 0.40 mmol/g , respectively.²⁵

It is possible to obtain higher vanadium loadings in vanadia–silica systems,^{25,26} as the solubility of the vanadium acac complex improved by dissolving the complex in toluene at higher temperature. However, it was checked that when warm toluene was used no higher metal loading was obtained for the mesoporous titania samples.

Figure 1 shows the N_2 adsorption–desorption isotherms at $-196\text{ }^{\circ}\text{C}$ for the blank mesoporous titania and $\text{VO}_x/\text{mesoporous titania}$ sample. The isotherms are type IV according to IUPAC classification and exhibit a H1 hysteresis loop, which is typical for mesoporous materials.²⁷

The isotherms of the calcined mesoporous titania and its grafted analogue exhibit a sharp increase in the adsorbed N_2 volume at $P/P_0 \approx 0.65$, characteristic for capillary condensation

within the uniform mesopores of the materials. The isotherm of the modified sample slightly decreases due to the vanadium present on the support (Figure 1), as it can be shown in Table 1 where the porosity of modified samples slightly decrease compare to the blank support.

However, the $\text{VO}_x/\text{meso Ti}$ sample shows the same type of hysteresis, which indicates that the deposition of vanadium oxides and the subsequent calcination did not induce a collapse of the mesostructure. Both samples show narrow pore size distribution with a maximum pore diameter of 46 \AA , even after deposition of VO_x .

Figure 2 shows FTIR–PAS spectra of blank mesoporous titania thermally treated at $300\text{ }^{\circ}\text{C}$ in air flow (Figure 2a), precursor with low and high concentrations of V-acac (parts b and c of Figure 2, respectively), and final $\text{VO}_x/\text{meso Ti}$ catalyst (Figure 2d).

Between 3900 and 3500 cm^{-1} the vibrations due to the OH groups of the mesoporous material are presented. The spectrum of the blank mesoporous titania shows two different vibrations, one at 3740 cm^{-1} , which corresponds to the more basic OH groups, and one at 3680 cm^{-1} , assigned to more acid OH groups. The band at 3740 cm^{-1} is assigned to the anatase phase.²⁸

After deposition of V-acac (parts b and c of Figure 2), a clear decrease of the OH bands is observed. It is obvious from the spectra that V-acac complexes are first preferentially attached to the more acid OH as the band at 3680 cm^{-1} almost disappeared even at low V concentration. At higher concentration, most of the OH groups have disappeared, only a small band assigned to the more basic OH group still remained, probably due to the steric hindrance caused by the bulky V-acac complex. The spectra of the precursors show the characteristic acac vibrations in the region $1600\text{--}1300\text{ cm}^{-1}$, which will be further studied in detail by transmission IR. After calcination at $300\text{ }^{\circ}\text{C}$ in airflow, the OH groups reappear, although the intensity has slightly decreased. The acac ligands are removed

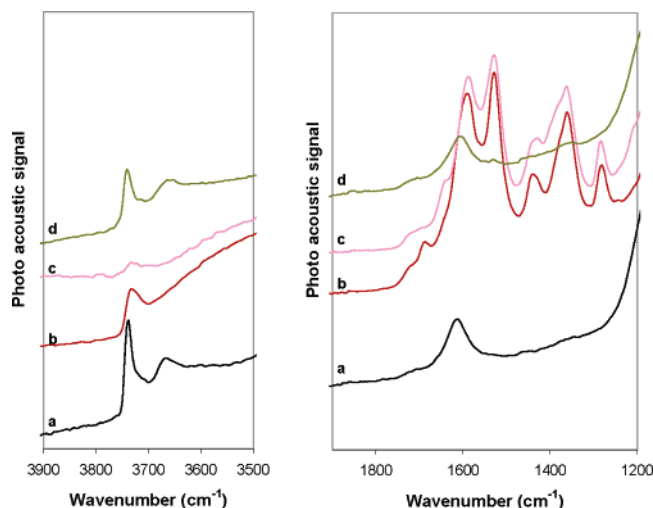


Figure 2. FTIR-PAS spectra of calcined mesoporous titania blank (a), precursor V-acac/meso TiO₂ with low concentration (0.10 mmol/g) (b), high concentration (0.40 mmol/g) of V-acac complex (c), and final VO_x/meso TiO₂ catalyst (d).

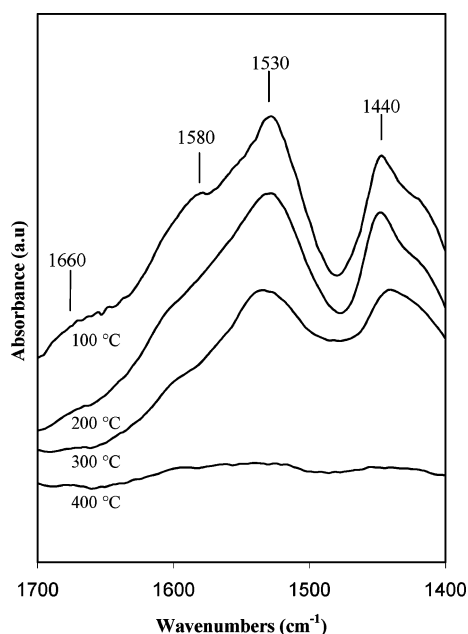


Figure 3. Thermal conversion process of a V-acac/meso TiO₂ catalyst in function of calcination temperature.

under calcination, upon the formation of a final VO_x/meso TiO₂ catalyst (Figure 2d).

The decomposition of the anchored complexes on the mesoporous TiO₂ support and the conversion of the physisorbed species toward covalently bond VO_x/TiO₂ were studied by using an in situ IR transmission cell. Transmission IR seems to be the appropriate spectroscopic technique to follow the calcination process in working conditions.

Figure 3 shows the spectra of VO(acac)₂ complex deposited on the mesoporous titania supported material in function of the calcination temperature.

These spectra show bands at 1660, 1580, 1530, and 1440 cm⁻¹. The band at 1660 cm⁻¹ is indicative of the presence of V-acac surface species, disappearing at 200 °C.²² The other bands present at 1580, 1530, and 1440 cm⁻¹, remaining up to higher temperatures, and not disappearing at 200 °C as in the case of V-acac, are assigned to Ti-acac. At 400 °C all the organics are removed, yielding the final VO_x/meso TiO₂ catalyst.

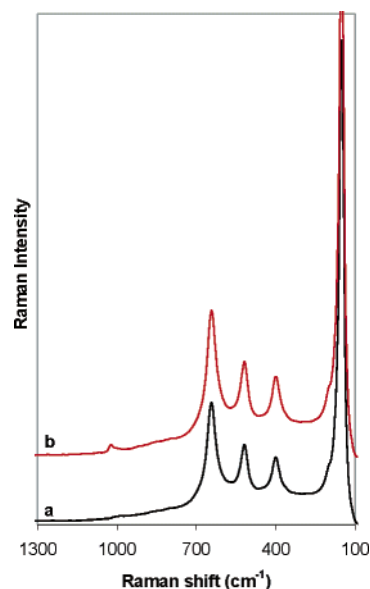


Figure 4. FT Raman spectra of the VO_x/meso TiO₂ with low V loading (0.10 mmol V/g) (a) and high V loading (0.40 mmol V/g) (b).

Further information on the structure of the grafted support is given by FT Raman spectroscopy (Figure 4). Raman spectra of calcined VO_x/meso TiO₂ show bands at 650, 520, 400, and 150 cm⁻¹. These are typical bands attributed to anatase crystals. These signals are very strong, so the bands assigned to V are low in intensity but present at 1030 cm⁻¹ and attributed to tetrahedral isolated V species.

The diffuse reflectance UV-vis spectra of catalysts with different amounts of VO_x (0.10 and 0.40 mmol V/g) are shown in parts a and b of Figure 5, respectively. All samples were measured in the dehydrated state (after drying the samples at 200 °C).

The spectrum of the blank mesoporous titania shows two bands, one at ~250 nm assigned to octahedral isolated titania (due to the contribution of amorphous titania) and a band at 330 nm assigned to anatase crystal phase.²⁹

Figure 5a shows the UV-vis-DR spectrum and its deconvolution of catalyst with a low V concentration (0.10 mmol/g). It shows bands centered at 250 and 330 nm (due to the contribution of mesoporous titania) but also a peak centered at 300 nm, assigned to tetrahedral isolated V species. Figure 5b presents the spectrum of a catalyst with higher loading of V (0.40 mmol/g). Apart from the peaks observed in Figure 5a, there are also bands centered at 300, 350, and 410 nm, which evidence the presence of tetrahedral isolated, tetrahedral 1D chain and square pyramidal V species, respectively.

It is clear that, with increasing V loading, the presence of vanadium in the form of polymeric species becomes more significant.

Surface acidity of catalysts plays an important role in the majority of the catalytic processes. The concentration of acidic sites and their strength can be studied by NH₃-TPD.

The results of the NH₃-TPD measurements obtained for blank mesoporous titania as well as for the titania modified with different amounts of vanadia are presented in Figure 6.

Ammonia desorption patterns for all the studied samples are carried out in the temperature range of 140–560 °C. A broad desorption peak with maximum at about 280 °C was obtained for blank mesoporous titania. Deposition of vanadia on titania resulted in an increase of the surface concentration of chemisorbed ammonia and splitting of the desorption patterns into two peaks centered at about 210 and 370 °C. The relative

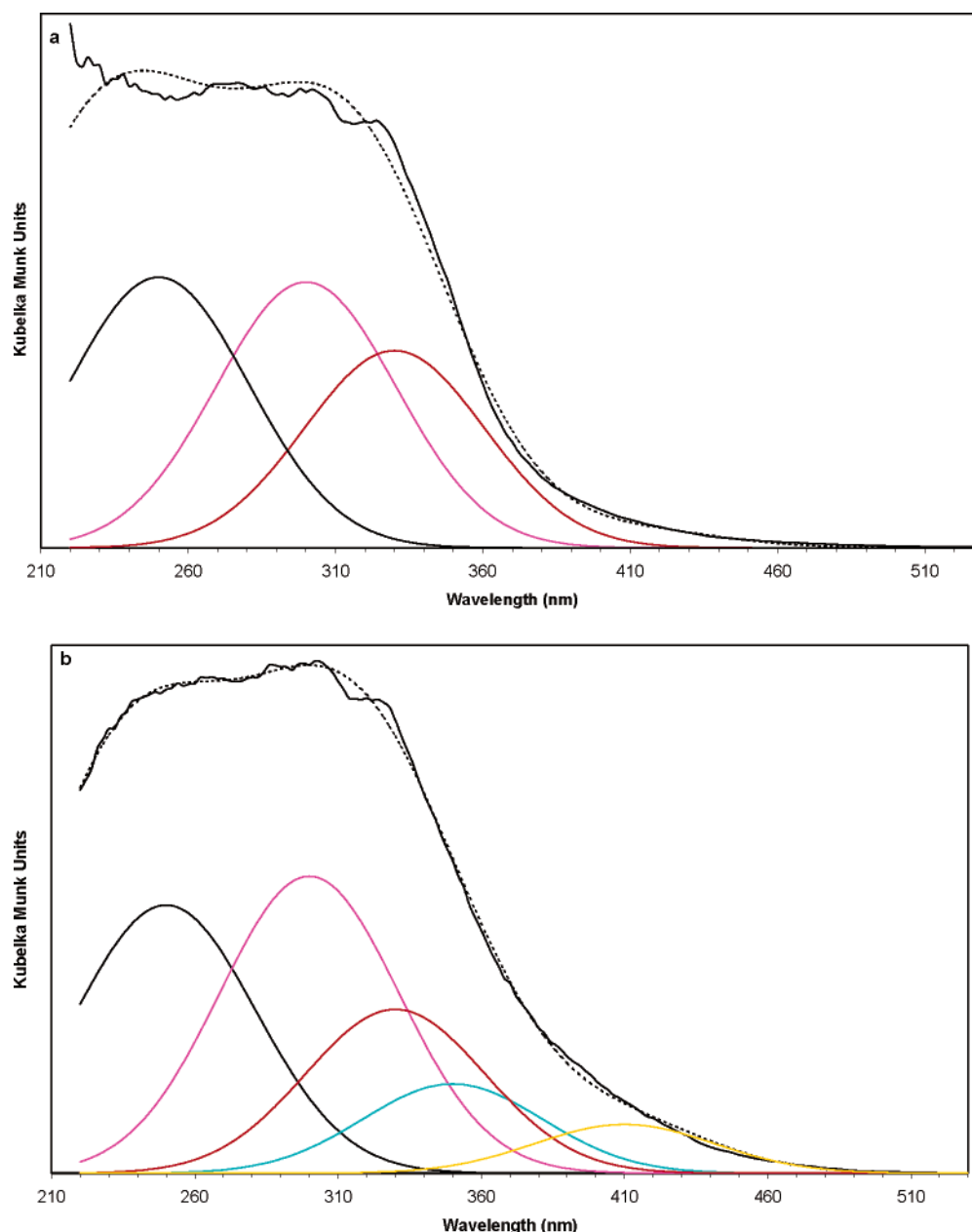


Figure 5. Diffuse reflectance UV-vis spectra of $\text{VO}_x/\text{meso TiO}_2$ with low V content (0.10 mmol/g) (a) and with high V content (0.40 mmol/g) (b).

intensity of these peaks depended on the quantity of vanadia deposited on the titania support. Stronger acidic sites, represented by the maximum of NH_3 desorption centered at 370 °C, dominated in the case of the sample containing lower amounts of deposited VO_x . An increase in the quantity of introduced vanadia resulted in a decrease of the surface concentration of acidic sites, which are characterized by a lower acidic strength.

It has been confirmed by UV-vis-DR that in samples with low V concentration (0.10 mmol V/g) vanadium in the isolated VO_x species dominates, while for the catalysts with a higher vanadium loading (0.40 mmol V/g) also significant amounts of oligomeric vanadia species are present. Thus, it could be concluded that ammonia molecules are probably significantly stronger chemisorbed on monomeric VO_x than on oligomeric vanadium species.

The results of the FTIR spectroscopic measurements of samples pretreated with ammonia presented by Busca et al.^{30,31} showed that pure TiO_2 -anatase exhibited only Lewis acidity, while for vanadia both Lewis and Brønsted acid sites were

found. Surface vanadyl species give rise to Lewis acid sites, which can be converted by water molecules into Brønsted centers. Ammonia molecules chemisorbed on Lewis acid centers are thermally more stable than ammonium ions.³² The broad temperature range, in which ammonia desorbs from the surface of the pure mesoporous titania suggests the presence of Lewis centers that are characterized by various acidic strength. Deposition of vanadia on the TiO_2 support generated additional acid centers (Lewis and Brønsted); however it seems that the catalyst with higher V loading contains more Brønsted acid sites than that with a lower vanadium content.

The mesoporous titania modified with VO_x were tested as catalysts for the selective reduction of NO with ammonia.

Figure 7 shows the results of the activity tests performed for the blank mesoporous titania and a series of different V-loading mesoporous titania catalysts (samples 1, 2, and 3, containing 0.10, 0.36, and 0.40 mmol V g⁻¹, respectively). The pure mesoporous titania is catalytically active in the high-temperature region. Modification of the TiO_2 support with vanadia signifi-

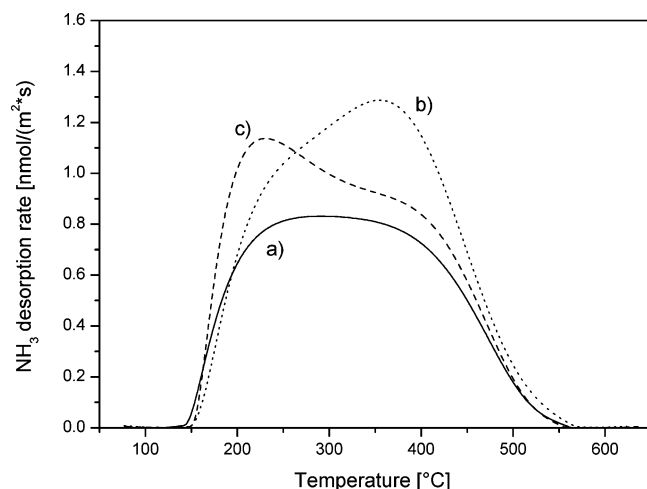


Figure 6. NH₃-TPD profiles obtained for blank mesoporous titania (a), VO_x/mesoporous titania with low V loading (0.1 mmol/g) (b), and VO_x/meso TiO₂ with high V loading (0.4 mmol/g) (c).

cantly increased the NO conversion at lower temperatures. It should be noticed that there is a correlation between V loading and activity of the catalysts. In general, an increase in amount of vanadia deposited on titania enhanced the activity of the catalysts in the low temperature range. A decrease in the NO conversion, observed in the high-temperature region, is related to the competitive reaction of ammonia oxidation by oxygen. It should be noticed that the V loading strongly influences this process. The lowest rate of ammonia oxidation was measured for the pure TiO₂ support, while an increase in the vanadia content increased the rate of this process. The decrease in the NO conversion observed in the high-temperature range ($T > 400$ °C) is attributed to the oxidation of ammonia by oxygen.

Figure 8 presents the specific rate of the NO conversion measured for the catalysts with different V loadings. The reaction rate increases with an increase in V content; however, there is not a linear correlation between these parameters. It should be noticed that V species present in the samples with the higher transition metal loading are catalytically more active than those in the catalyst with a lower vanadium content. The UV-vis-DR measurements have shown the presence of monomeric and polymeric V species; however the contribution of the later one is higher in the samples with the high vanadium content. Went et al.^{33–35} and Busca et al.³⁶ reported that the reactivity of such polymeric species is higher than that of isolated vanadyls, due to superior redox properties. Also Nova et al.³⁷ studied the deactivation of a DeNO_x commercial catalyst, observing that polymeric vanadium species present higher activity in the SCR reaction compared to monomeric vanadium species.

Therefore, it could be concluded that not only V loading but also a type of the introduced vanadium species is responsible for the activity of the catalysts in the DeNO_x process.

Figure 9 presents results of the stability test performed over mesoporous titania modified with 0.40 mmol V/g at temperature 395 °C. It should be noticed that only small changes in the NO conversion and selectivity toward N₂ was observed during 25 h of the catalytic test.

In Figure 10 are shown results of the catalytic tests performed with increasing and decreasing reaction temperature. It should be noticed that the NO conversions measured in the test with increasing temperature is significantly higher than those recorded in test with decreasing temperature. Therefore, it could be concluded that the catalyst was deactivated at higher temper-

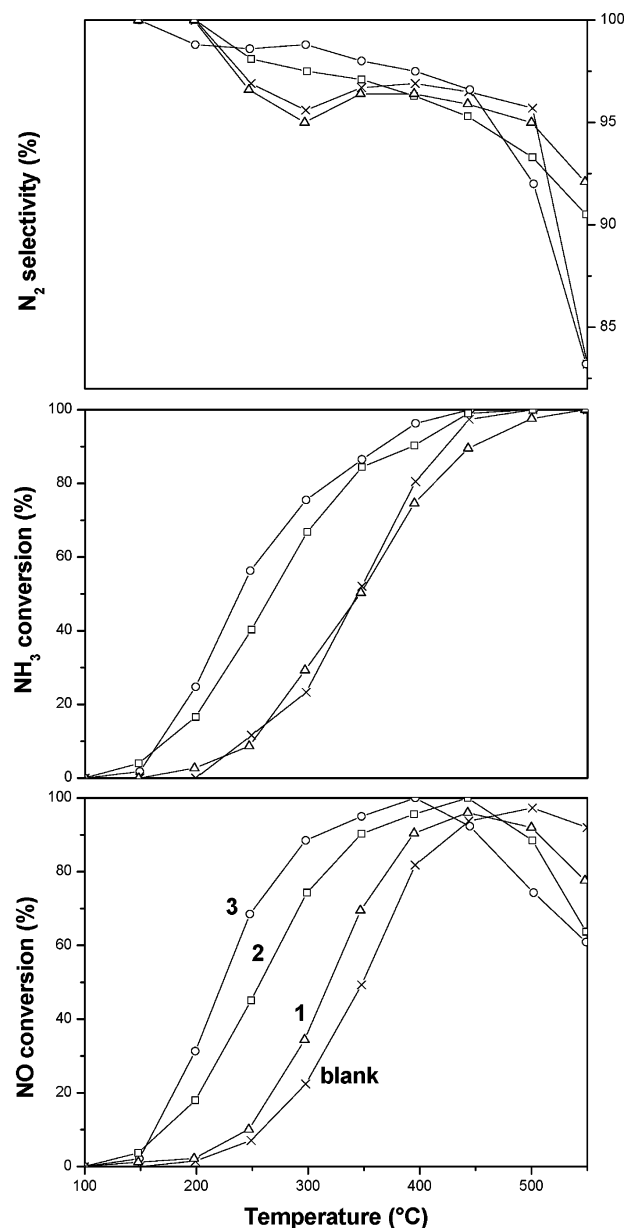


Figure 7. Catalytic activity data of the blank mesoporous titania and VO_x/meso TiO₂ catalysts having different V content: (1) 0.10 (▲), (2) 0.36 (■), and (3) 0.40 (●) mmol V/g.

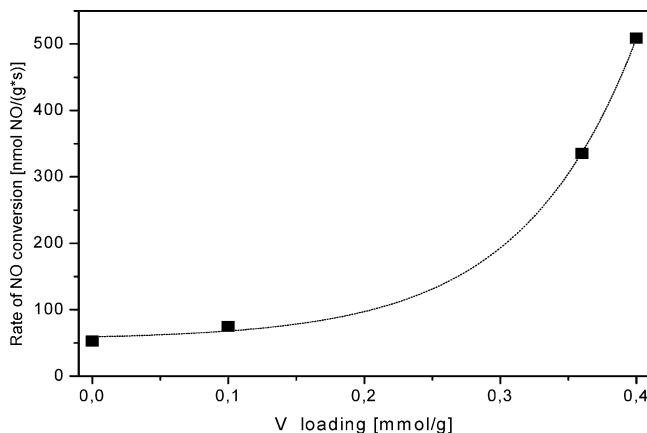


Figure 8. Specific rate of NO conversion obtained for different loadings of vanadium at temperature 250 °C.

atures ($T > 400$ °C). This effect is probably related to slightly structural changes of the mesoporous titania support. By

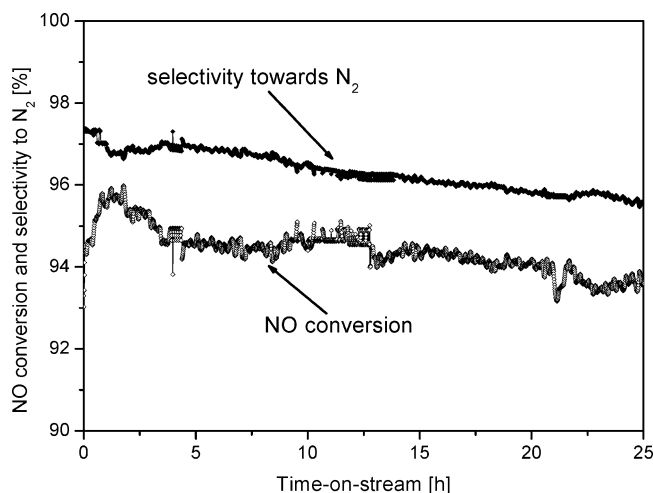


Figure 9. Stability test performed for the mesoporous titania modified with 0.40 mmol V/g at temperature 395 °C.

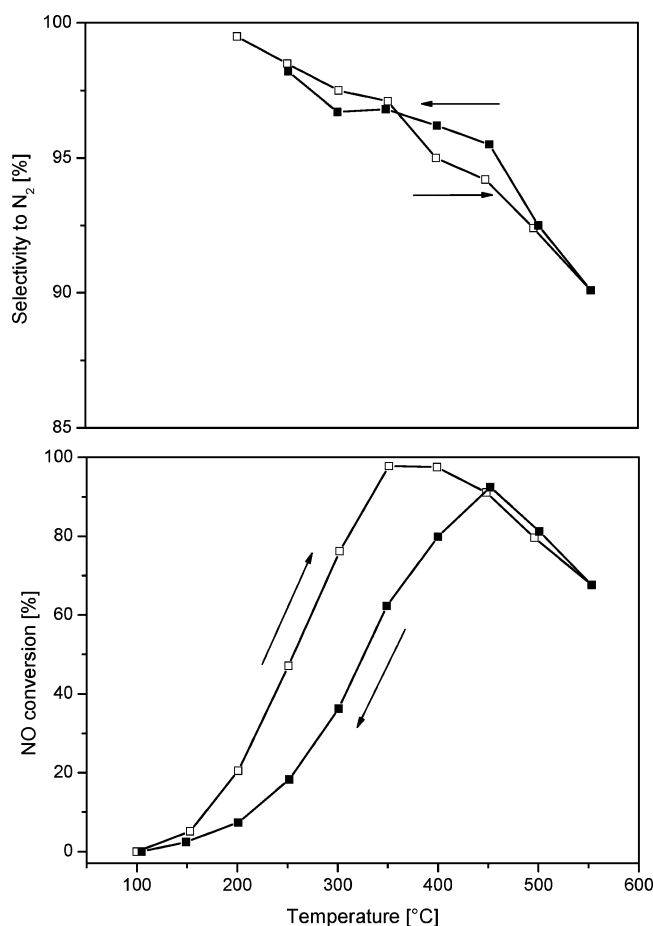


Figure 10. Catalytic test with increasing and decreasing reaction temperature performed for mesoporous titania modified with 0.36 mmol V/g.

comparison of results presented in Figures 9 and 10, it could be concluded that the studied catalytic materials are stable to temperature 400 °C. At higher temperatures partial deactivation of the catalyst takes place.

The influence of water vapor on the catalytic performance of mesoporous titania modified with 0.40 mmol V/g was studied by periodical catalytic tests with dry and wet reaction mixture (Figure 11). After the first exchange from dry to wet reaction mixture, the NO conversion decreased about 2%. The subse-

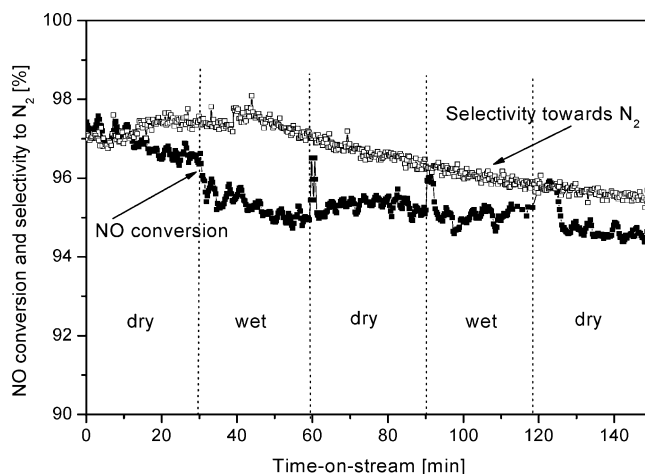


Figure 11. Catalytic test with dry and wet reaction mixture for mesoporous titania modified with 0.40 mmol V/g.

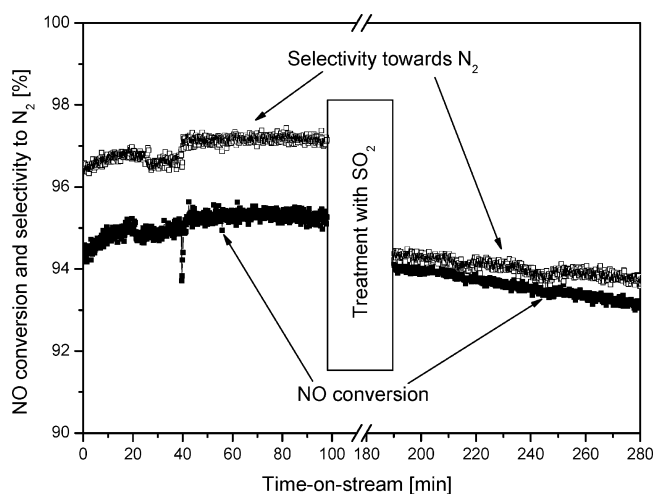


Figure 12. Study of the influence of SO₂ on the catalytic performance of mesoporous titania modified with 0.40 mmol V/g.

quent introductions of water vapor into the reaction only slightly influenced the activity of the catalyst.

It has been reported³⁷ that polymeric vanadium species present higher activity in the oxidation of SO₂ to SO₃.

Figure 12 presents results of the studies of SO₂ influence on the performance of the catalyst. After 100 min of the catalytic test performed at 395 °C, a flow of the reaction mixture was exchanged for a flow of SO₂ (0.2 vol. %) diluted in helium. The treatment with SO₂ was performed at 395 °C for 90 min. Then, a flow of the SO₂-containing mixture was exchanged for a flow of reaction mixture. The catalytic test was performed at 395 °C for an additional 90 min. After treatment with SO₂, the NO conversion decreased only by 1.5%, while selectivity to N₂ decreased by about 3%.

Therefore, it can be concluded that, even if polymeric vanadium species are active in the SO₂ oxidation reaction, the influence is not very significant.

Oxidation of SO₂ to SO₃ is the next problem, which should be avoided in the case of a DeNO_x catalyst. This process was studied over the VO_x/meso TiO₂ (0.10 mmol V/g) catalyst at 400 °C. Results of this experiment are presented in Figure 13. It shows that the formation of SO₃ as well as consumption of O₂ was detected. Therefore, it could be concluded that the studied samples do not catalyze oxidation of SO₂ to SO₃.

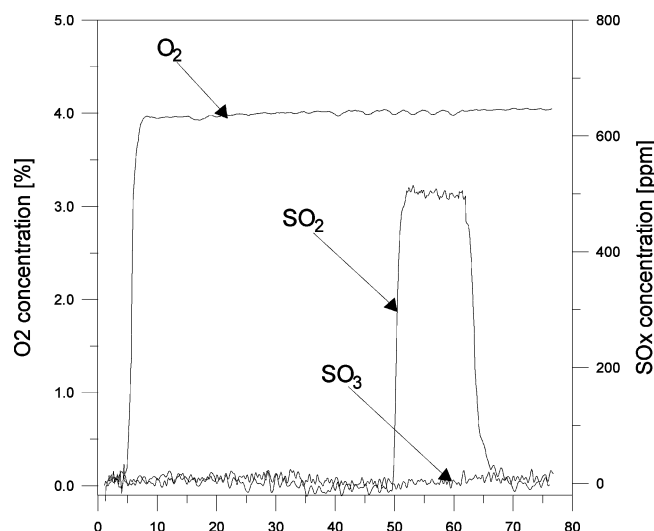


Figure 13. Test of SO_2 oxidation over the $\text{VO}_x/\text{meso TiO}_2$ (0.10 mmol V/g) catalyst ($T = 400^\circ\text{C}$, 100 mg of sample, 4 vol. % of O_2 , 500 ppm SO_2 , rest He, total flow 50 mL/min).

4. Conclusions

Mesoporous titania was successfully synthesized, obtaining a thermally stable (up to $\sim 500^\circ\text{C}$) mesostructure with a surface area of about $\sim 350\text{ m}^2\text{ g}^{-1}$. Vanadium oxide species were successfully deposited onto the mesoporous titania surface by the MDD method. FT Raman spectra show that vanadium in $\text{VO}_x/\text{mesoporous titania}$ is present as isolated species, without the presence of vanadia clusters. In addition, UV-vis-DR reveals also the presence of polymeric species, especially in samples with high vanadium loadings. A detailed porosity analysis was carried out to prove that, when the catalysts obtained after vanadium deposition and subsequent calcination at 300°C in air flow, no changes were observed in their mesostructure and their porosity characteristics. These samples were as catalysts for the SCR of NO_x . They show great activity for the NO conversion, reaching 100% in the range of $350\text{--}400^\circ\text{C}$. At higher temperatures, the NO conversion decreased due to oxidation of NH_3 by oxygen. The activity increases with increasing V loading, because of the higher contribution of polymeric V species. It should be noticed that typical DeNO_x converts operates in the temperature range of $300\text{--}400^\circ\text{C}$, therefore a decrease in the catalytic activity observed above this temperature range does not exclude possible commercial application of these type of catalysts for the DeNO_x process. Additional advantage of the mesoporous titania modified with vanadium is their resistance toward water vapor. Sulfur dioxide only slightly influenced the NO conversion and selectivity to N_2 .

Acknowledgment. The authors thank the EC (NoE Inside Pores), the Ministry of Flanders, and the Polish Ministry of Scientific Research and Information Technology for financial support in the frame of bilateral Flemish-Polish project for

2004-2005. P.C. also acknowledges the Fund for Scientific Research—Flanders for financial support. Mr. K. Walgraeve is acknowledged for the aid in part of the experimental work.

References and Notes

- (1) Fornes, V.; Lopez, C.; Lopez, H. H.; Martinez, A. *Appl. Catal.* **2003**, *249*, 345.
- (2) Lakshmi, J. L.; Ihasz, N. J.; Miller, J. M. *J. Mol. Catal.* **2001**, *165*, 199.
- (3) Zhang, Q.; Wang, Y.; Ohishi, Y.; Shishido, T.; Takehira, K. *J. Catal.* **2001**, *202*, 308.
- (4) Miller, J. M.; Lakshmi, L. *J. Appl. Catal. A* **2000**, *190*, 197.
- (5) Kim, Y. H.; Lee, H. *Bull. Korean Chem. Soc.* **1999**, *20*, 1457.
- (6) Chatterjee, M.; Iwasaki, T.; Hayashi, H.; Onodera, Y.; Ebina, T.; Nagase, T. *Chem. Mater.* **1999**, *11*, 1368.
- (7) Fierro, J. L. G.; Arrua, L. A.; Lopez Nieto, J. M.; Kremenec, G. *Appl. Catal.* **1988**, *37*, 323.
- (8) Roussel, H.; Mehloakulu, B.; Belhadji, F.; Van Steen, E.; Millet, J. M. *J. Catal.* **2002**, *205*, 97.
- (9) Handy, B. E.; Baiker, A.; Schraml-Marth, M.; Wokaun, A. *J. Catal.* **1992**, *133*, 1.
- (10) Caraba, R. M.; Masters, S. G.; Eriksen, K. M.; Parvulescu, V. I.; Fehrmann, R. *Appl. Catal. B* **1991**, *34*, 191.
- (11) Lin, C.; Bai, H. *Appl. Catal. B* **2002**, *1*, 1306.
- (12) Jung, S. M.; Grange, P. *Appl. Catal. B* **2002**, *36*, 325.
- (13) Lietti, L.; Alemany, J. L.; Forzatti, P.; Busca, G.; Ramis, G.; Giamello, E.; Bregani, F. *Catal. Today* **1996**, *29*, 143.
- (14) Antonelli, D. M.; Ying, J. Y. *Angew. Chem., Int. Ed. Engl.* **1995**, *34*, 2014.
- (15) On, D. T. *Langmuir* **1999**, *15*, 8561.
- (16) Antonelli, D. M. *Microporous Mesoporous Mater.* **1999**, *30*, 315.
- (17) Yang, P.; Zhao, D.; Margolese, D. I.; Chmelka, B. F.; Stucky, G. *Nature* **1998**, *396*, 152.
- (18) Cassiers, K.; Linssen, T.; Mathieu, M.; Bai, Y. Q.; Zhu, H. Y.; Cool, P.; Vansant, E. F. *J. Phys. Chem. B* **2004**, *108*, 3713.
- (19) Baltes, M.; Van Der Voort, P.; Weckhuysen, B. M.; Rao, R. R.; Catana, G.; Schoonheydt, R. A.; Vansant, E. F. *Phys. Chem. Chem. Phys.* **2000**, *2*, 2673.
- (20) Van Der Voort, P.; Baltes, M.; Vansant, E. F. *J. Phys. Chem. B* **1999**, *103*, 10102.
- (21) Schrijnemakers, K.; Vansant, E. F. *J. Porous Mater.* **2001**, *8*, 83.
- (22) Segura, Y.; Cool, P.; Van Der Voort, P.; Mees, F.; Meynen, V.; Vansant, E. F. *J. Phys. Chem. B* **2004**, *108*, 3794.
- (23) Grosso, D.; de A. A. Soler-Illia, G. J.; Babonneau, F.; Sanchez, C.; Albouy, P.-A.; Brunet-Bruneau, A.; Balkenende, A. R. *Adv. Mater.* **2001**, *13*, 1085.
- (24) Vogel, Arthur I. *Quantitative Inorganic Analysis*, 3rd ed.; Longman: London, 1971; p 790.
- (25) Segura, Y.; Cool, P.; Kustrowski, P.; Chmielarz, L.; Dziembaj, R.; Vansant, E. F. *J. Phys. Chem. B* **2005**, *109*, 12071.
- (26) Meynen, V.; Segura, Y.; Mertens, M.; Cool, P.; Vansant, E. F. *Microporous Mesoporous Mater.* **2005**, *85*, 119.
- (27) De Boer, J. H.; Linsen, B. G.; Osinga, T. J. *Catal.* **1964**, *4*, 643.
- (28) Primet, M.; Pichat, P.; Mathieu, M. *J. Phys. Chem.* **1971**, *75*, 1216.
- (29) Chiker, F.; Nogier, J. Ph.; Launay, F.; Bonardet, J. L. *Appl. Catal. A* **2003**, *240*, 309.
- (30) Busca, G.; Saussey, H.; Saur, O.; Lavalley, J. C.; Lorenzelli, V. *Appl. Catal.* **1985**, *14*, 245.
- (31) Ramis, G.; Busca, G.; Lorenzelli, V. P.; Forzatti, P. *Appl. Catal.* **1990**, *64*, 243.
- (32) Rajadhyaksha, R. A.; Knözinger, H. *Appl. Catal.* **1990**, *64*, 243.
- (33) Went, G. T.; Leu, L.-J.; Bell, A. T. *J. Catal.* **1992**, *134*, 479.
- (34) Went, G. T.; Leu, L.-J.; Rosin, R. R.; Bell, A. T. *J. Catal.* **1992**, *134*, 492.
- (35) Went, G. T.; Leu, L.-J.; Lombardo, S. L.; Bell, A. T. *J. Phys. Chem.* **1992**, *96*, 2235.
- (36) Busca, G.; Lietti, L.; Ramis, G.; Berti, F. *Appl. Catal. B* **1998**, *18*, 1.
- (37) Nova, I.; dall'Acqua, L.; Lietti, L.; Giamello, R.; Forzatti, P. *Appl. Catal. B* **2001**, *35*, 31.